

STUDY OF STRUCTURAL, AND ANTIBACTERIAL PROPERTIES OF $\text{Fe}_x\text{Mn}_{(1-x)}\text{O}_3$ NANOPARTICLES PREPARED BY MICROWAVE ASSISTED PRECIPITATION TECHNIQUE

Dr. L. Jayaselvan¹, Dr. T.S. Jayanthi², Dr. A. Prabumarachan³

¹Assistant professor, Department of Physics, Vivekananda college, Agasteeswaram-629701. Affiliated to Manonmaniam Sundaranar University, Thirunelveli, Abishekapatti, Tamilnadu, India

²Associate professor, Department of Physics, Vivekananda college, Agasteeswaram-629701. Affiliated to Manonmaniam Sundaranar University, Thirunelveli, Abishekapatti, Tamilnadu, India

³Assistant professor, Department of Physics, Vivekananda college, Agasteeswaram-629701. Affiliated to Manonmaniam Sundaranar University, Thirunelveli, Abishekapatti, Tamilnadu, India,

E-mail: jjphy1982@gmail.com

Abstract

The Fe doped Mn_2O_3 nanoparticles were synthesized by the microwave-assisted method and synthesized samples were further annealed at 500°C and the samples were subjected to analyze structural and Phase Analysis properties. The structural properties of the nanoparticles were characterized by using X-ray diffractometry. XRD pattern revealed that the existence of Mn_2O_3 with cubic structure and Mn-doped Fe is a rhombohedral lattice structure. The Raman analysis confirms the phase formation of the prepared samples.

1. INTRODUCTION

Fe_2O_3 nano materials have a wide variety of applications among the metal oxides based systems. It is most widely studied materials in recent literature due to their impressive properties and magnetic strength and its ability to utilize technologies such as in biotechnology, electrochemistry, catalysis, magnetism and biomedicine. [1-3], in meticulous Fe_2O_3 nanoparticles have concerned momentous concentration for prospective applications in electronics [4] fuel cells [5]. Manganese oxide is non stoichiometry composite when it is doped by ferric ion. In the Fe doped manganese oxide has various applications including magnetic property, dielectric, catalytic, dissolution, electrochemical and electromagnetic absorbance. Manganese oxide is an ideal oxidizing agent it is used to remove the toxic contaminants from the drinking water [6]. In the nanoparticles research, size dependent is an important property. It plays a main roll in tailoring properties [7]. Fe doped manganese oxide nanoparticles considered to exist mainly typical spinel structure tetrahedral sites with 80% are occupied by Mn^{2+} ions [8]. It is also having insulating properties with a very small gap [9]. Warner et al. investigated Mn-doped Fe_3O_4 nanoparticles use of heavy metal origin as of aqueous solutions [10]. Recent years in particular renewed attention in hematite $\alpha\text{-Fe}_2\text{O}_3$ nanoparticles [11-13]. Hence in this chapter the preparation of Fe doped Mn_2O_3 nanoparticles and its structural, optical and morphological properties were discussed.

2. EXPERIMENTAL PROCEDURE

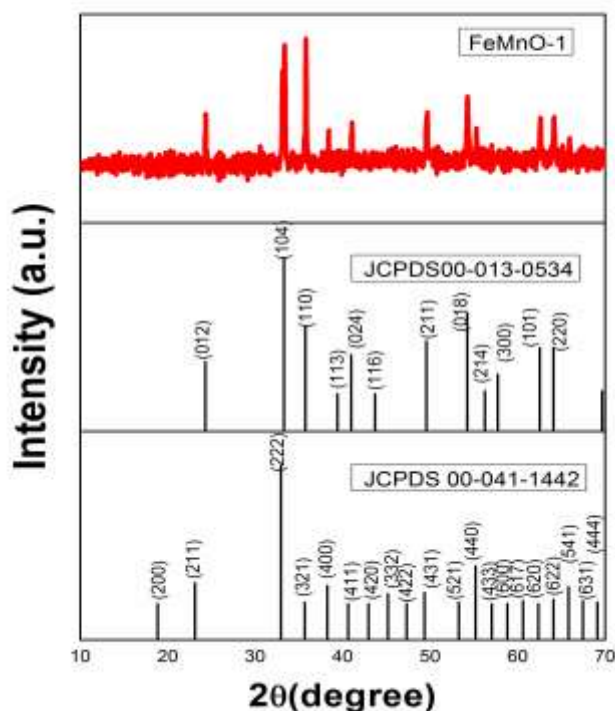
Among the available methods simple microwave assisted synthesis method has been chosen because this method is less expensive and an efficient technique for the preparation of transition metal oxides. In this method heat can be transferred easily to the solution and the heating temperature can be selected precisely.

In the present study $\text{Fe}_x\text{Mn}_{(1-x)}\text{O}_3$ nano powder were prepared from the aqueous solution of MnCl_2 and FeCl_2 . FeMnO-1 nano powder were prepared from the aqueous solution of FeCl_2 (0.2 M), MnCl_2 (0.8 M) reduced by NaOH (1M). In this process, required amount FeCl_2 and MnCl_2 powder were added to 100ml distilled water in a round bottom flask and then the NaOH pellets were slowly added in to the above solution resulted solution was kept under constant stirring for an hour to form a brown colour solution. The solution thus obtained was heated in a domestic microwave oven (540 W, 92°C) for 20 minutes. After microwave processing, the mixture was cooled to room temperature and the resulted brown precipitate was separated by centrifugation followed by repeated washing with distilled water and absolute ethanol to remove the impurities and residual materials. After washing, the nano particles were dried at 60°C . Finally, the prepared materials were annealed at 500°C for three hours. The same procedure is repeated to dope with Fe in various proportions FeMnO-2 (MnCl_2 0.60 and FeCl_2 0.40), FeMnO-3 (MnCl_2 0.40 and FeCl_2 0.60), FeMnO-4 (MnCl_2 0.20 and FeCl_2 0.80) and FeMnO-5 (FeCl_2 1M). Thus $\text{Fe}_x\text{Mn}_{(1-x)}\text{O}_3$ powder was prepared for $x = 0.2, 0.4, 0.6, 0.8$ and 1M. Prepared samples were named as FeMnO-1 , FeMnO-2 , FeMnO-3 , FeMnO-4 and FeMnO-5 .

3.RESULT AND DISCUSSION

3.1 Structural Analysis

X-Ray diffraction is very important tool used for extracting information recording microstructure like space group, lattice type, unit cell, unitcell volume, structural imperfections, crystalline size etc. The crystalline size and lattice parameter are very important factor which would be extracted from the XRD



peak width analysis.

Fig.1 X-ray diffraction pattern of $\text{Fe}_x\text{Mn}_{(1-x)}\text{O}_3$ sample prepared with $x=0.2$

The role of dopant in individual nanostructures becomes more significant in the doped sample FeMnO-1 with $x=0.2$ ($\text{Fe}_{0.2}\text{Mn}_{0.8}\text{O}_3$). Fig.1 shows the XRD pattern of FeMnO-1 sample. It reveals that the sample is a composite consisting of Mn_2O_3 and Fe_2O_3 phase. This could be understood on matching the peaks for the JCPDS Standards 00-013-0534 and 00-041-1442. The Mn_2O_3 phase is cubic and the Fe_2O_3 phase is in rhombohedral lattice. Calculated unit cell parameters and other related structural parameters are listed in Table 1.

The unit cell edges of both cubic Mn_2O_3 ($a=9.396 \text{ \AA}$) and rhombohedral Fe_2O_3 ($a=4.96 \text{ \AA}$ and $c=13.825 \text{ \AA}$) are almost equal and they are comparable with the standard JCPDS values ($a=9.409 \text{ \AA}$), ($a=5.031 \text{ \AA}$ and $c=13.737 \text{ \AA}$). Other related structural parameters like unit cell volume and density are calculated respectively for both phases. The crystallite size and micro strains values are almost the same for the two phases.

Fig 2 shows the XRD pattern of $\text{Fe}_x\text{Mn}_{(1-x)}\text{O}_3$ sample prepared with $x=0.4, 0.6$ and 0.8 . From the obtained results it is revealed that the prominent peaks correspond to reflections (012), (104), (110), (024), (113), (116), (018), (214) and (300) planes in perfect 2θ locations of rhombohedral phase of FeMnO_3 as that of the standard JCPDS data [JCPDS Card No: 00-013-0534]. Moreover the

FeMnO_3 phase with rhombohedral structure belongs to the space group $R\bar{3}c$ and space group number = 167. The structural parameters of all the samples were calculated and listed in the Table 1.

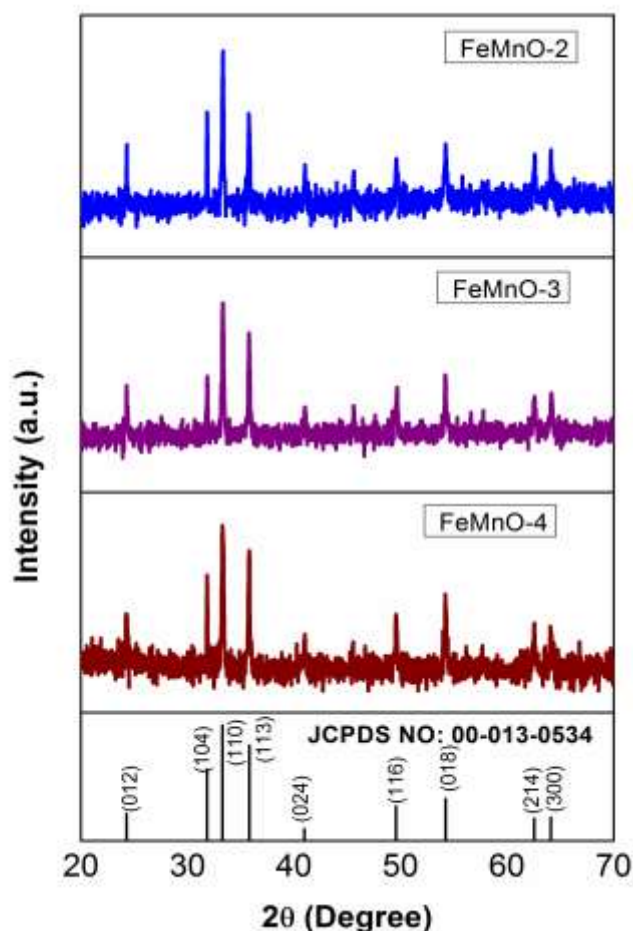


Fig.2 XRD patterns of $\text{Fe}_x\text{Mn}_{(1-x)}\text{O}_3$ sample prepared with $x=0.4, 0.6$ and 0.8

In all the samples the lattice parameter values are almost the same and are comparable with the JCPDS values. So the unitcell volume and the density are almost the same. However, the crystalline size increase initially with x values and the decreases the variation of microstrain follows similarly.

In the sample FeMnO-5 , x value is fixed at 1 mole (1M) and the peak appearing at 2θ range of $33.28^\circ, 35.74^\circ, 49.49^\circ, 54.23^\circ, 62.26^\circ$ and 64.17° can be attributed to the plane (104), (110), (024), (116), (214) and (300) respectively. The crystalline structures of the corresponding sample is Hematite iron oxide nanoparticles in Rhombohedral structure ($a=b$ $a=5.0280$, $c=13.700$) space group $R\bar{3}c$ and space group number 167. The peaks are perfectly matched using Cell Cal software and are found in match with the standard values (00-001-1053). The Mn and Fe have several oxidation states. The ionic radius of Fe^{2+} ions is 0.78 \AA and Fe^{3+} ions is 0.645 \AA . At the same time Mn ions have smaller ionic radius (Mn^{2+} - 0.58 \AA , Mn^{3+} - 0.66 \AA and Mn^{4+} - 0.53 \AA) than the Fe ions [14-15]. The lattice parameter and the crystal size of the Fe doped nanoparticles are higher than that of pure Mn_2O_3 nanoparticles. This result confirmed the expansion of lattice parameter due to the doping of Fe ions in to the Mn lattice. The Mn ions ionic radius is smaller than Fe^{2+} ions. The Fe^{2+} ions might be dominant as the assimilation of material among upper ionic radius will enlarge the lattice, thus raising the particle size [16]. No specific progression in lattice parameter is observed in the Fe doped nanoparticles by the raise in Fe doping. This might be due to the existence of several oxidation states in Mn and Fe; this controls the lattice reduction and lattice expansion of the samples. The unit cell volume is the dependent parameter to lattice constant and so its variation is similar to that of lattice constant. Obtained density values are high than that of the bulk value. The decrease of elastic strain is observed with an increase in particle size the both (crystallite size and micro strain) are having inverse dependency.

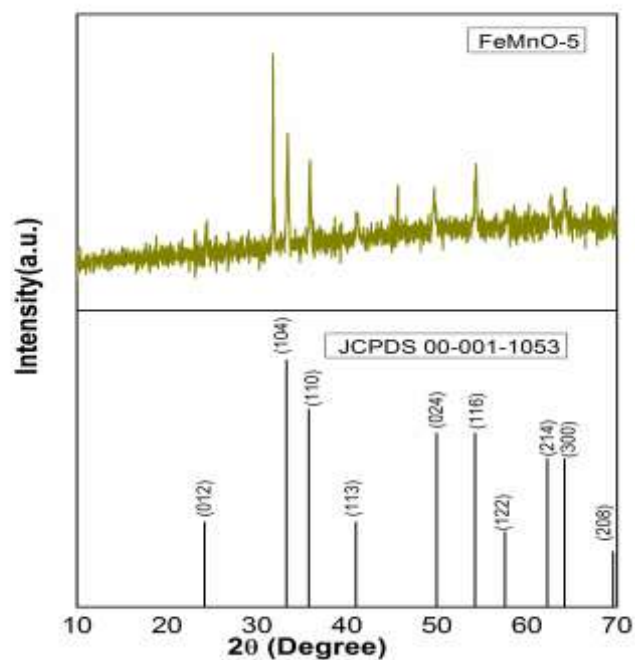


Fig.3X-ray diffraction pattern of $\text{Fe}_x\text{Mn}_{(1-x)}\text{O}_3$ sample with $x=1\text{M}$

Table.1 Structural parameters of pure and Fe Doped Mn_2O_3 nano particles

Sample Details	Lattice Parameter (Å)		Volume (Å) ³		Density (g/cm ³)		Crystalline Size (nm)	Strain x 10 ⁻³
	Exp	Std	Exp	Std	Exp	Std		
FeMnO (Cubic)	a=9.396	a=9.409	818.58	833	5.12	5.03	38.28	0.675
FeMnO-1 (rhombohedral)	a=4.96 c=13.82 5	a=5.031 c=13.737	294.67	301.11	5.39	5.27	39.88	0.239
FeMnO-2	a=5.026 c=13.68 9	a=5.031 c=13.737	299.54	301.11	5.30	5.27	45.93	0.847
FeMnO-3	a=5.022 c=13.70 7	a=5.031 c=13.737	299.50	301.11	5.31	5.27	60.72	0.634
FeMnO-4	a=5.027 c=13.69 7	a=5.031 c=13.737	299.81	301.11	5.30	5.27	47.18	0.821
FeMnO-5	a=5.011 c=13.67 4	a=5.028 c=13.730	297.47	300.60	5.34	5.26	38.13	1.11

3.3 METAL-OXIDE PHASE ANALYSIS USING RAMAN

Raman spectroscopy is the dominant and all-round characterization instrument for determining the semiconductor devices of nano scale and chemical composition analysis of the substance. Raman scattering spectrum was taken in the range from 50-1500 cm^{-1} . The Raman spectra of the prepared samples were displayed in Fig. 4. In the FeMnO-1 sample the observed peaks are placed at 183, 305, 629 and 694 cm^{-1} the first peak 183 cm^{-1} confirms to the presence of manganese oxide [17]. The observed little peak at 612 cm^{-1} corresponds to phonon mode (E_g) and it confirms the presence of Fe ions [18-19]. The another two broad peaks at 305 and 694 cm^{-1} are in A_{1g} Raman active modes. These two main peaks are principally accredited the presence of Mn_2O_3 group and symmetric stretch of vibration mode [20-21]. This result confirmed that the sample FeMnO-1 is in mixed phase of both (Fe and Mn). On increase the doping concentration $x = 0.4$ to 0.8 (FeMnO-2 to FeMnO-4) the observed peaks are shifted to the lower wave number region and the samples are having Fe and Mn mixed phase. The FeMnO-5 sample is a pure Fe_2O_3 sample the observed bands 610, 490, 400, 282 and 217 cm^{-1} are confirm the presence of Fe_2O_3 [22-23]. The A_{1g} modes are assigned to 217 and 490 cm^{-1} Raman bands and the E_g modes are assigned at 610, 400 and 282 cm^{-1} band. The main band at around 1310 cm^{-1} is dispensed to a two-magnon dissipating which emerges from the connection of two magnons made on antiparallel close turn destinations [24-26].

Table.2 Previously reported-Raman analysis results of Fe_2O_3

Reference	Raman shift (cm^{-1})
Verble et al. [27]	680, 560, 420, 320, 300
Boucherit et al. [28]	670, 550
Hart et al. [29]	676, 550, 472, 420, 320, 298
Dunnwald and Otto. [30]	1322, 676, 550, 470, 418, 319, 298
Ohtsuka et al. [31]	665, 540
Thierry et al. [32]	670, 550
de Faria et al. [33]	662.7, 533.6, 301.6
Gasparov et al. [34]	670, 540, 308, 193
Degiorgi et al. [35]	672, 542, 462, 410, 318, 160
Graves et al. [36]	706, 570, 490, 336, 226
Romcevic and Kostic. [37]	665, 540, 311
Gupta et al. [38]	669, 540, 410, 300
Present study	629, 694, 282, 400, 490, 610, 130

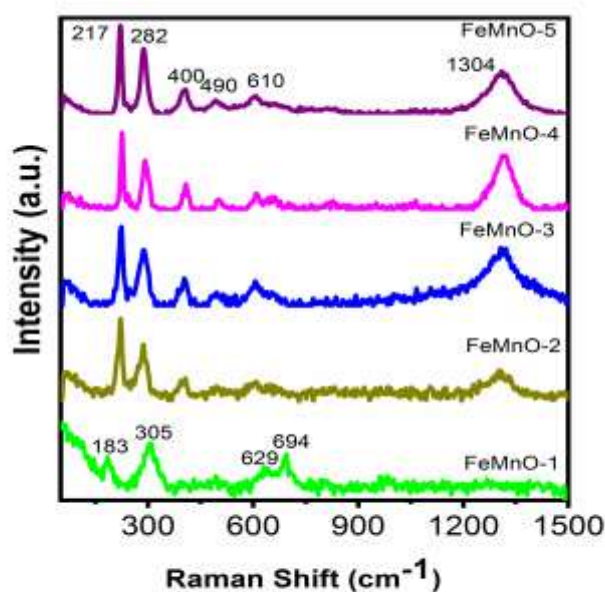


Fig.4. Raman Spectra of FeMn₂O₃ nano particles

at 723.47 eV. This signifies the presence of Fe³⁺ ions in the prepared Fe₂O₃ sample [39-40]. The iron oxide nanoparticles have very high binding energy value comparable to any other metal oxides [41]. In addition the two weak Fe³⁺ shake satellite peaks are observed at 716.73 eV and 731.07 eV. The Fe2p_{3/2} satellite band is appeared around 8 eV this same result have reported by Clara Pereira et al [42]. The spin orbit split value (2p_{3/2}-2p_{1/2}) is 14.8 eV. All the experiential results are analogues to XRD results that proved the Fe₂O₃ nanoparticles formation of with no any other impurities.

Conclusion

In summary, smooth and compact FeMn₂O₃ nanoparticles were prepared by microwave assisted synthesis method. The structural variations with various concentrations of the prepared nanoparticles were analyzed. The strong absorption bands are appears around ~ 345 and ~ 530 nm. The absorption spectrum of Fe doped nanoparticles is due to the d-d conversion among higher e_g and lowers t_{2g} of the Mn ion

REFERENCE

- [1] Lemine, O M, Ghiloufi, I, Bououdina, M, Khezami, L, M'hamed, M &Taha, A 2014, 'Nanocrystalline Ni doped α -Fe₂O₃ for Adsorption of Metals from Aqueous Solution', Journal of alloys and compounds, vol. 588, pp.592–595.
- [2] Monica Barroso, Alexander Cowan, J, Stephanie Pendlebury, R, Michael Graezel, DavidKlug, R & James Durrant, R 2011, 'The Role of Cobalt Phosphate in Enhancing the Photocatalytic Activity of α -Fe₂O₃ toward Water Oxidation', Journal of American Chemical Society, vol. 113, pp. 14868–14871.
- [3] Challarapu Venkataramana, Balaji Anjaneyulu, R, Jhansi Rani Sunkara & Muralikrishna, R 2019, 'Visible light Responsive Photo catalytic Activity of Pd/Fe₂O₃ Nanoparticles for Congo red dye Degradation', Journal of Applicable Chemistry, vol.8, no. 1, pp. 419- 424.
- [4] Ramachandra Rao, CN, Giridhar Kulkarni, U, John Thomas, P & Peter Edwards, P 1999, 'Metal nanoparticles and their assemblies', Chemical Society Reviews, vol. 29, pp. 27- 35.
- [5] Vismadeb Mazumder, Youngmin Lee & Shouheng Sun 2010, 'Recent Development of Active Nanoparticle Catalysts for Fuel Cell Reactions', Advanced Functional Materials, vol. 20, pp. 1224-1231.
- [6] Amjad Khan, Arbab Mohammad Toufiq, Fawad Tariq, Yaqoob Khan, Rafaqat Hussain, Naureen Akhtar & Shams ur Rahman 2019, 'Influence of Fe doping on the Structural, Optical and Thermal Properties of α -MnO₂ Nanowires', Materials Research Express, vol. 6, no.6, pp. 1-15.
- [7] An-Hui Lu, Salabas, E L & Ferdi Schth 2007, 'Magnetic Nanoparticles Synthesis Protection Functionalization, and application', Angewandte Chemie International Edition, vol. 46, pp. 1222-1244.
- [8] Julius Hastings, M & Lester Corliss, M 1956, ' Neutron Diffraction Study of Manganese Ferrite' , Physical Review, vol. 104, no. 8, pp. 324-328.
- [9] Szotek, Z, Temmerman, W M, Kodderitzsch, D, Svane, A, Petit, L & Winter, H 2006, 'Electronic structures of normal and inverse spinel ferrites from first principles' , Physical Review B, vol. 74, no. 174431, pp. 1-11.
- [10] Cynthia Warner, L, Wilaiwan Chouyyok, Katherine Mackie, E, Doinita Neiner, Laxmikant Saraf, V, Timothy Droubay, C, Marvin Warner, G & Shane Addleman, R 2012, 'Manganese doping of magnetic iron oxide nanoparticles: tailoring surface reactivity for a regenerable heavy metal sorbent' , Langmuir, vol. 28, pp. 3931-3937.
- [11] Deraz, N M & Alarifi, A 2012, 'Novel processing and magnetic properties of hematite/maghemite nano-particles', Ceramics International, vol. 38, no. 5, pp. 4049-4055.
- [12] Adinaveen, T, Vijaya, J J & Kennedy, L J 2014, 'Studies on the structural, morphological, optical, and magnetic properties of α -Fe₂O₃ nanostructures by a simple one-step low temperature reflux condensing method', Journal of Superconductivity and Novel Magnetism, vol. 27, pp. 1721-1727.
- [13] Lu, H M & Meng, X K 2010, ' Morin temperature and Néel temperature of hematite nanocrystals', The Journal of Physical Chemistry C, vol. 114, pp. 21291-21295.
- [14] Hernandez, WY, Tsampas, MN, Zhao, C, Boreave, A, Bosselet, F & Vernoux, P 2015, "La/Sr-based perovskites as soot oxidation catalysts for Gasoline Particulate Filters," Catal. Today, vol. 258, pp. 525–534.

- [15] Li, F, Zhang, L, Evans, DG & Duan, X 2004, “Structure and surface chemistry of manganese-doped copper-based mixed metal oxides derived from layered double hydroxides,” vol. 244, pp. 169–177.
- [16] Aneggi, E, Cabbai, V, Trovarelli, A & Goi, D 2012, “Potential of Ceria-Based Catalysts for the Oxidation of Landfill Leachate by Heterogeneous Fenton Process,” *International Journal of Photoenergy*, vol. 2012, pp. 1-8.
- [17] Tao Gaoa, Helmer Fjellvåga and Poul Norbya 2009, ‘A comparison study on Raman scattering properties of α - and β -MnO₂’, *Analytica Chimica Acta*, vol. 648, pp. 235–239.
- [18] Bersani, D, Lottici, P & Montenero, A 1999, ‘ Raman scattering characterization of gel-derived titania glass’, *Journal of Raman Spectroscopy*, vol. 30, pp. 355-360.
- [19] Xu, YY, Zhao, D, Zhang, XJ, Jin, WT, Kashkarov, P & Zhang, H 2009, ‘ Synthesis and characterization of single-crystalline α -Fe₂O₃ nanoleaves’, *Physica E*, vol.41, pp. 806–811.
- [20] Ji-Yu Wang, Pan-Yong Kuanga, Nan Lia, Zhao-Qing Liua, Yu-Zhi Sua & Shuang Chen 2015, ‘ Facile hydrothermal synthesis of cobalt manganese oxides spindles and their magnetic properties’, *Ceramics International*, vol. 41, no. 7, pp. 8670-8679.
- [21] Leilei Lan, Quanjun Li, Guangrui Gu, Huafang Zhang & Bingbing Liu 2015, ‘Hydrothermal synthesis of γ -MnOOH nanorods and their conversion to MnO₂, Mn₂O₃, and Mn₃O₄ nanorods’, *Journal of Alloys and Compounds*, vol. 644, pp. 430-437.
- [22] Liqun Wang, Xuegang Lu, Chang Han, Ruie Lu, Sen Yang & Xiaoping Song 2014, ‘Electrospun hollow cage-like α -Fe₂O₃ microspheres: synthesis, formation mechanism, and morphology-preserved conversion to Fe nanostructures’, *Crystal Engineering Communications*, vol. 16, pp. 10618–10623.
- [23] Houda Mansour, Hanen Letifi, Radhouane Bargougui, Sonia De Almeida Didry, Beatrice Negulescu Cecile Autret-Lambert, Abdellatif Gadri & Salah Ammar 2017, ‘Structural, optical, magnetic and electrical properties of hematite (α -Fe₂O₃) nanoparticles synthesized by two methods polyol and precipitation’, *Applied Physics A*, vol. 123, no. 12, pp. 1-10.
- [24] Bashir Ahmmad, Kwati Leonard, Shariful Islam, M d, Junichi Kurawaki, Manickavachagam Muruganandham, Takahiro Ohkubo & Yasushige Kuroda, 2013, ‘Green synthesis of mesoporous hematite (α -Fe₂O₃) nanoparticles and their photocatalytic activity’, *Advanced Powder Technology*, vol.24, pp. 160–167.
- [25] Liqiao Chen, Xianfeng Yang, Jian Chen, Jia Liu, Hao Wu, Hongquan Zhan, Chaolun Liang & Mingmei Wu 2010, ‘ Continuous Shape- and Spectroscopy-Tuning of Hematite Nanocrystals’, *Inorganic Chemistry*, vol. 49, pp. 8411–8420.
- [26] McCarty, K F 1988, ‘Inelastic Light Scattering In α -Fe₂O₃: Phonon Vs Magnon Scattering’, *Solid State Communications*, vol. 68, no. 8, pp. 799-802.
- [27] Larry Verble, J 1974, ‘Temperature-dependent light-scattering studies of the Verwey transition and electronic disorder in magnetite’, *Physical Review B*, vol. 9, no. 12, pp. 5236-5248.
- [28] Boucherit, N, Hugot-Le Goff, A & Joiret Raman, S 1991, ‘ studies of corrosion films grown on Fe and Fe-6Mo in pitting conditions’, *Corrosion Science*, vol. 32, no. 5–6, pp. 497-507.
- [29] Hart, T R, Adams, S B, Tempkin, H, Balkanski, M, Leite, R & Porto, S 1976, ‘Proceedings of the 3rd International Conference on Light Scattering in Solids’, Flammarion, Paris, pp. 254–258.
- [30] Dunnwald, J, Otto, A 1989, ‘ An investigation of phase transitions in rust layers using Raman spectroscopy’, *Corrosion Science*, vol. 29, no. 9, 1989, pp. 1167-1176.
- [31] Ohtsuka, T, Kubo, K & Sato, N 1986, ‘Raman spectroscopy of thin corrosion films on iron at 100 to 150 C in air’, vol. 42, no. 8, pp. 476-481.
- [32] Thierry, D, Persson, D, Leygraf, C, Boucherit, N & Hugot-Le Goff, A 1991, ‘Raman spectroscopy and XPS investigations of anodic corrosion films formed on Fe-Mo alloys in alkaline solutions’, *Corrosion Science*, vol. 32, no. 3, pp. 273-284.
- [33] De Faria, D L A, Venancio Silva, S & de Oliveira, M T 1997, ‘Raman micro spectroscopy of some iron oxides and oxyhydroxides’, *Journal of Raman Spectroscopy*, Vol. 28, pp. 873–878.
- [34] Gasparov, L V, Tanner, D B, Romero, D B, Berger, H, Margaritondo, G & Forro, L 2000, ‘Infrared and Raman studies of the Verwey transition in magnetite’, *Physical Review B*, vol. 62, pp. 7939–7944.
- [35] Degiorgi, L, Blatter-Morke, I & Wachter, P 1987, ‘Magnetite Phonon modes and the Verwey transition’, *Physical Review B*, vol. 35, pp. 5421–5424.

- [36] Graves, P R, Johnston, C & Campaniello, J J 1988, 'Raman scattering in spinel structure ferrites', *Materials Research Bulletin*, vol. 23, no. 11, pp. 1651–1660.
- [37] Romcevic, N, Kostic, R, Romcevic, M, Hadzic, B, Kuryliszyn-Kudelska, I, Dobrowolski, W, Narkiewicz, U & Sibera, D 2008, 'Raman Scattering from ZnO (Fe) Nanoparticles', *Acta Physica Polonica A*, vol. 114, no. 5, pp. 1323-1328.
- [38] Gupta, R, Sood, A K, Metcalf, P & Honig, J M. *Physical Review B*, vol. 65, no. 104430, pp. 1-8.
- [39] Kowalczyk, S P, Ley, L, McFeely, F R & Shirley, D A 1975, 'Multiplet splitting of the manganese 2p and 3p levels in MnF₂ single crystals', *Physical Review B*, vol. 11, no. 4, pp. 1721 - 1727.
- [40] Fadley, C S & Shirley, D A 1970, ' Multiplet Splitting of Metal-Atom Electron Binding Energies', *Physical Review A*, vol. 2, no. 4, pp. 1109-1120.
- [41] Cheng, C M, Huang, Y, Wang, N, Jiang, T, Hu, S, Zheng, B Z, Yuan, H Y & Xiao, D 2015, 'Facile fabrication of Mn₂O₃ nanoparticle-assemble hierarchical hollow spheres and their sensing for hydrogen peroxide', *ACS Applied Materials & Interfaces*, vol.7, pp. 9526–9533.
- [42] Cao, H Q, Wu, X M, Wang, G H, Yin, J F, Yin, G, Zhang, F & Liu, J K 2012, 'Biom mineralization strategy to α -Mn₂O₃ hierarchical nanostructures', *Journal of Physical Chemistry C*, vol. 116, pp. 21109-21115.